CURRENT COLLECTORS OPERATING IN HIGH MAGNETIC FIELDS

Prepared by

T.A. Aanstoos, R.W. Faidley, J.H. Gully, and M.L. Spann

Presented at

1987 International Current Collector Conference
Austin, TX

November 16-17, 1987

Publication PN-123

Center for Electromechanics
The University of Texas at Austin
Balcones Research Center
Bldg. 133, EME 1.100
Austin, TX 78758
512/471-4496

Original

CURRENT COLLECTORS OPERATING IN HIGH MAGNETIC FIELDS

T. A. Aanstoos, R. W. Faidley, J. H. Gully, M. L Spann
Center for Electromechanics
The University of Texas at Austin
Balcones Research Center
EME 1.100, Building 133
Austin, TX 78758-4497
(512) 471-4496

ABSTRACT

An air core, superconducting field coil, self motored, pulsed homopolar generator has been built and tested. This device uses multiple voltage generating passes and five Tesla magnetic field density to develop open circuit voltage of 500 V. Early testing of this machine showed that the original designs for the motoring and armature current collection systems failed during operation in high external fields.

Because this generator is similar to self excited, air core, improved energy devices in the requirement for current collection in high magnetic fields, new designs for both the motoring and armature brushgear systems were developed. A hinged mechanism is used to support the motoring brush, where the current is conducted by a laminated shunt. This design results in significant improvement in sensitivity to contact wear. The armature brushes are compensated in the region of the sliding contact itself, in order to minimize the effect on contact load. An idle (non-current carrying) trailing arm provides dynamic stability. Both designs have been analyzed for thermal and mechanical stability. Static prototypes have been built to verify overall spring rate and fabrication procedures. Dynamic testing of the motoring brush system is scheduled on a high speed contact test system, at slip speed, current density, and duration similar to rated performance in the high voltage homopolar generator.

Introduction

The high voltage homopolar generator is an air core, multiple spool, superconducting field coil, self motoring, high voltage device designed for powering electromagnetic accelerators without intermediate energy storage or conditioning. In two sequences of tests, problems arose with the current collection systems. First, excessive motoring brush drag, and the lack of a high current motoring power supply, prevented high speed operation of the generator. A redesigned set of motoring brushes and a 6,000 A dc power supply were installed.

In a second series of tests, the generator was excited to 4.9 T, motored to 4,000 rpm, and discharged at 90 kA peak current. However, both the motoring and armature brushgear sets failed. The motoring brushes, spring loaded and supported by radially cantilevered straps, apparently failed due to excessive wear of the copper-graphite sliding contact material. This wear resulted in a light load condition at the slip rings, since the brush strap spring rate dominated that of the compression coil spring used to develop contact load. Overheating resulted, and one or more sliding contacts failed at the strap braze joint. In the emergency discharge that followed, a fault current passed through the motoring brushgear, causing complete failure of the system.

The armature brushgear sets experienced problems at each rotor slip ring diameter. At the inner diameter, the brush straps were inadequately self-compensated for operation in the high external field of the machine. As a result, the contacts lifted from the slip ring, interrupting current and caus-

ing fracturing of the contact due to chattering. The outer rotor brushes were not compensated, but the current carrying brush straps failed in bending due to Lorentz body forces experienced at current levels well below design current.

Self excited, air core homopolar generators are similar to improved energy density homopolar generators in the requirement for conducting high current density discharge currents through regions of high external fields. Component development for such current collection systems at realistic current and field levels is difficult and expensive without a device such as the high voltage homopolar. For these reasons, redesign of the high voltage generator's current collection systems was undertaken in the course of conceptual design of an improved energy density, self excited, air core homopolar generator.

Both the primary (armature) and motoring brushgear sets have been redesigned. The motoring brushes are now of a hinged, laminated strap design that will be less sensitive to sliding contact wear. Prototypes of these brushes have been built and will be tested, at slip speed and current density comparable to the high voltage homopolar, in a sliding electric contact test system. The armature brushes are now of a compensated, idle trailing arm design. A laminated copper brush strap assembly allows for radial compliance for actuation, while the trailing arm provides mechanical stability without having to withstand electromagnetic forces. Prototypes of these brush designs have been built to verify fabrication and assembly techniques. In this paper, details of the design and analysis of these current collection systems are presented and discussed.

Description

A sectional view of the high voltage homopolar generator (HVHPG) is shown in figure 1. Four spool type, 7050-T736 aluminum rotors are installed by thermal shrink fit onto a 316L stainless steel shaft, and are insulated from the shaft and each other by plasma sprayed Al_2O_3 ceramic coatings. The rotor/shaft subassembly is contained by a 5052 aluminum stator, parted along the axial midplane, that encases the rotor in a clamshell fashion. The shaft is supported by two hydrostatic radial bearings and one double acting hydrostatic thrust bearing--these are housed in the stainless steel end plates. ETP 101 copper collector turns are machined from ring forgings and assembled into the stator cavities by dowels and fasteners. Each of these rings is insulated from the stator, except the outer collector ring at the number 1 rotor--this ring is electrically common with the stator, which serves as the discharge current path. This rotor also serves as the motoring armature--sliding face contacts ride on slip rings at two radial locations on the face of this rotor, which conducts motoring current from the 6,000 A external dc power supply. Primary armature brushgear sets at each diameter of each rotor connect the rotors in series. All face and rim slip rings are plasma sprayed with copper 0.051 cm thick. The assembled stator and rotors are inserted into the bore of the superconducting field coil. The generator is installed and tested at an external test site, as shown in figure 2. The technical parameters of the coil and the generator are given in table 1. A complete description of the HVHPG can be found in reference 1.

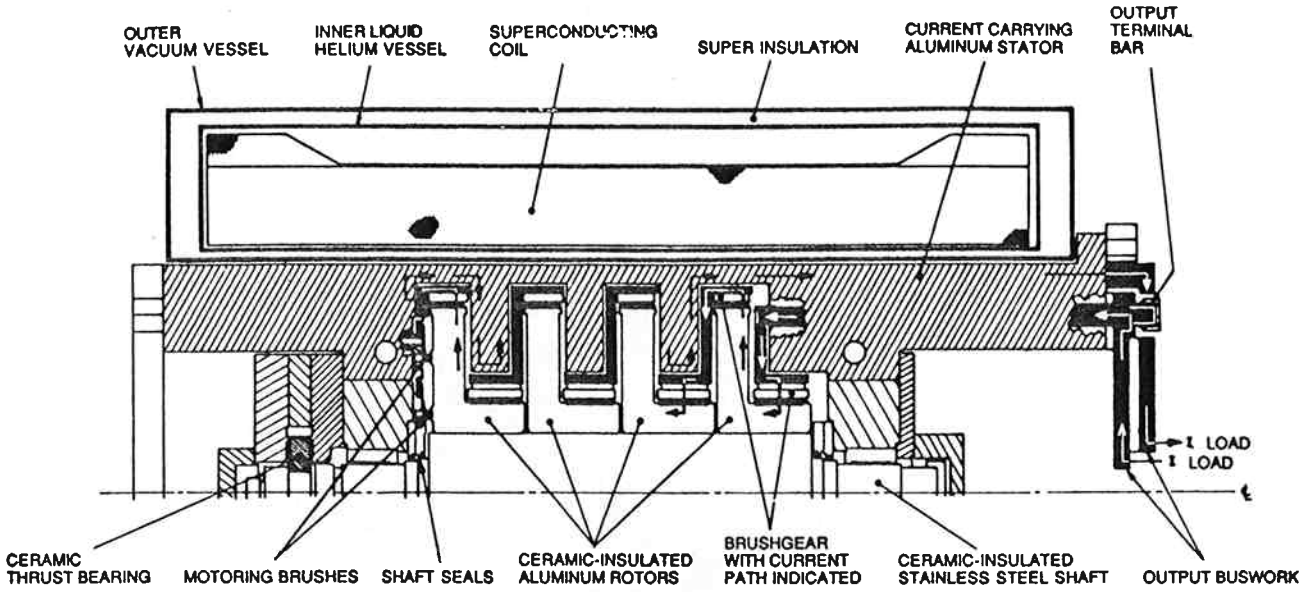

Figure 1. Sectional view of the high voltage homopolar generator

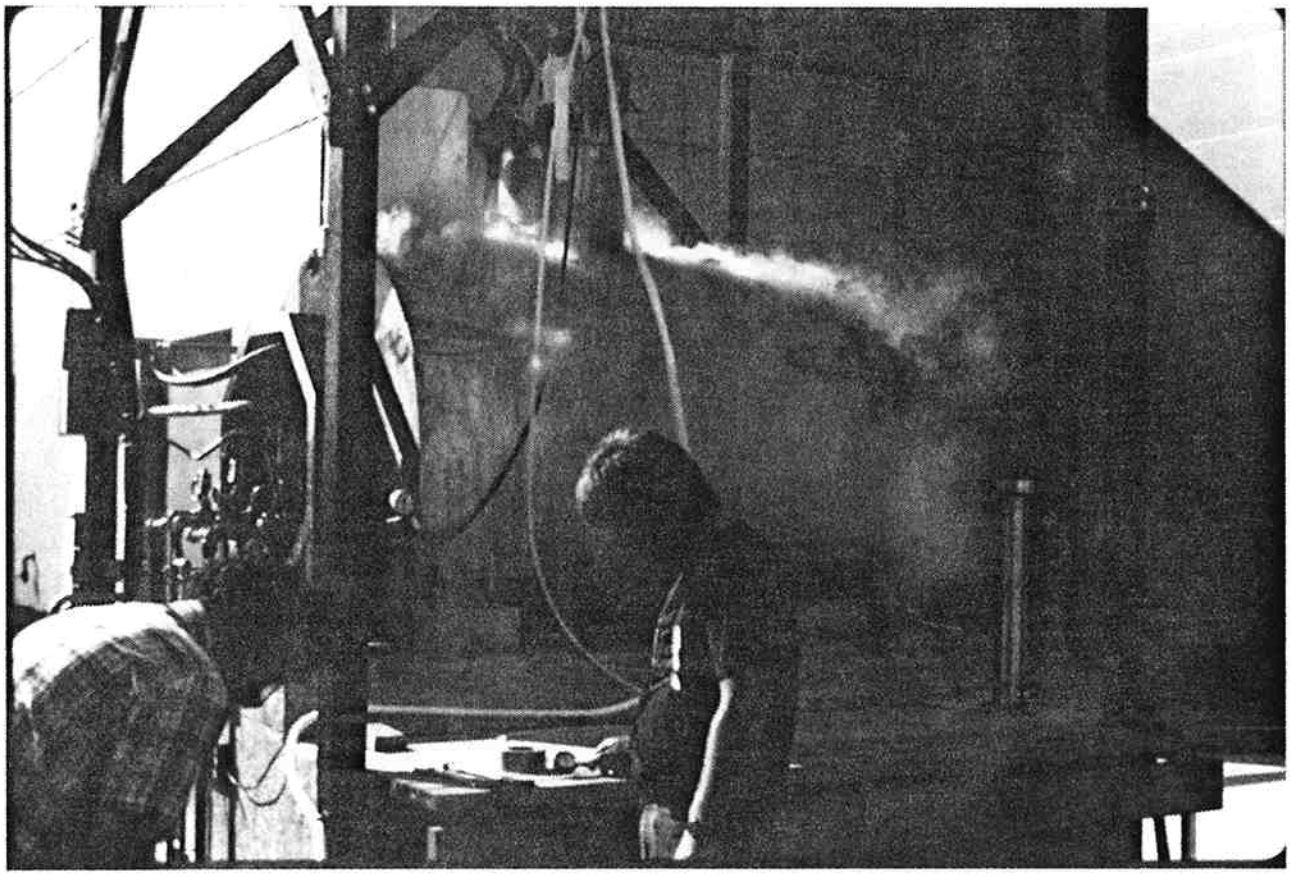

Figure 2. HVHPG installation

Table 1. High voltage homopolar generator technical parameters

TERMINAL VOLTAGE	500	V
EQUIVALENT CAPACITANCE	26	F
MAXIMUM ROTOR SPEED	694 6,627	s^{-1} rpm
MAXIMUM SLIP RING SPEED (OUTER)	220	m/s
ROTOR MASS MOMENT OF INERTIA	13.5	$kg\text{-}m^2$
MAXIMUM STORED ENERGY	3.25	MJ
MAXIMUM OUTPUT CURRENT (DESIGN)	700	kA
MAXIMUM AVERAGE FIELD DENSITY	5	T
COIL MMF	11.4×10^6	A-turns
STORED COIL ENERGY	12	MJ

Armature Current Collection System

Original Design

The original designs of the inner and outer armature brushes are shown in figures 3 and 4 respectively. The design characteristics of these brush systems are given in table 2. Both designs were based on traditional trailing arm brush strap configurations. In the inner rotor brushgear, the trailing strap was compensated by a return strap that was intended to contribute a self compensating force to counteract external field forces, which, at this location, act to decrease sliding contact load. This compensating force proved inadequate, resulting in current interruption, as described above. The resulting chatter caused transverse fractures in the heel region of some sliding contacts, as shown in figure 5. The outer brushgear used no compensating strap, since external forces here act to increase contact load. However, during the fault current that occurred at the end of phase 2 testing, the current carrying brush straps failed in bending due to this external force (fig. 6), at a current level well below design capability. Thus both brushgear sets were not designed adequately for conducting rated HVHPG discharge current at full excitation.

The forces on the original current collection components were calculated. Of special interest in any current collector is the normal (radial) reaction at the sliding contact to forces acting on all parts of the structure. In the original inner system, three major forces affected normal contact force: the actuator force (F_a), the reaction to the self-compensation force (F_b), and the reaction to the external force (F_e).

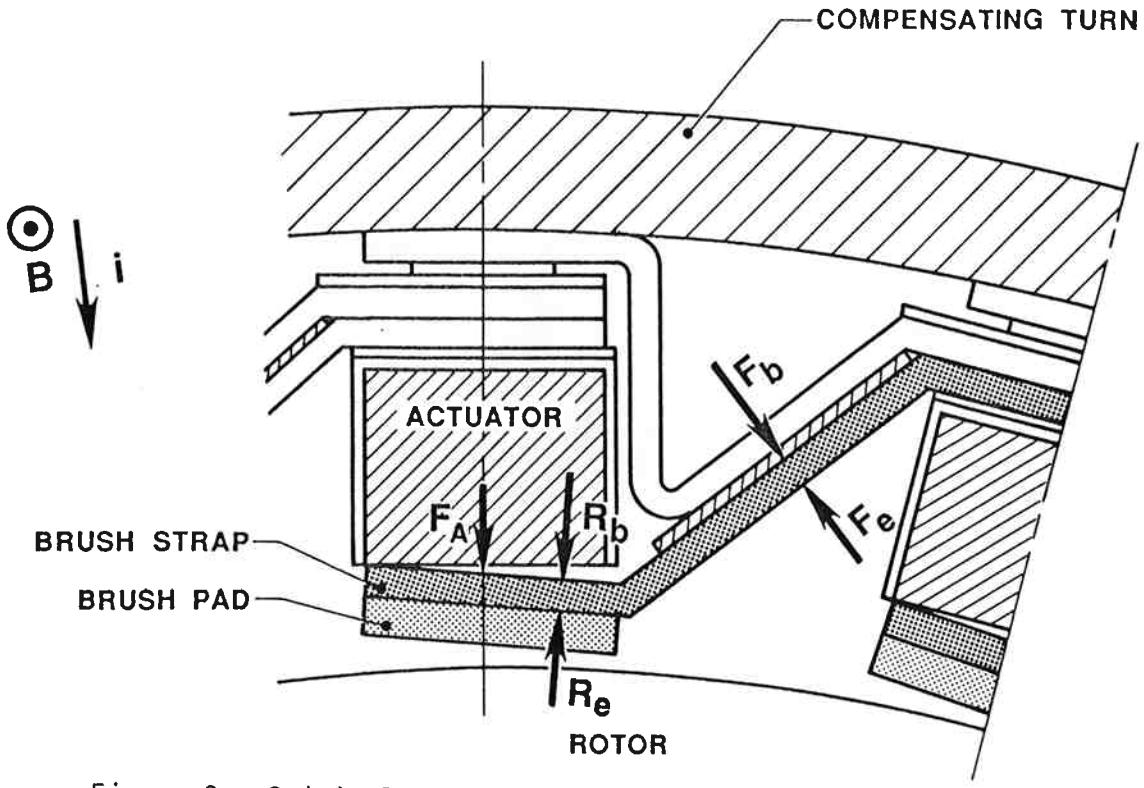

Figure 3. Original HVHPG inner armature brushgear design

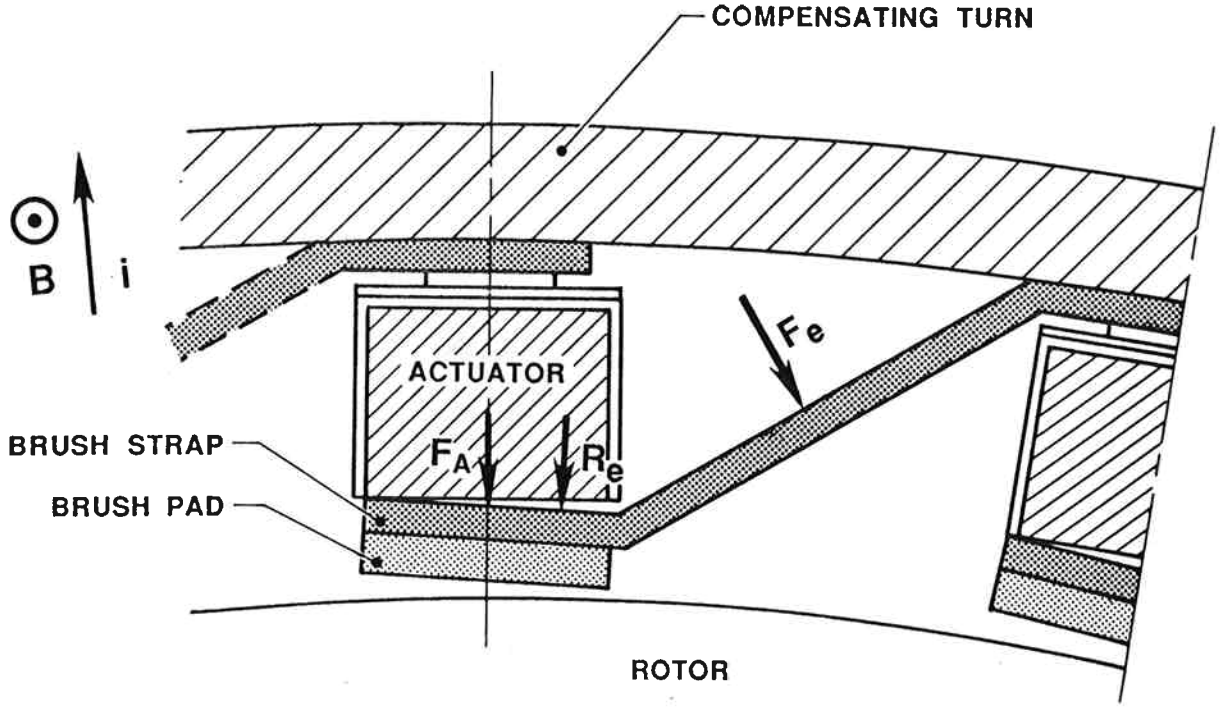

Figure 4. Original HVHPG outer armature brushgear design

Table 2. Original armature brushgear design characteristics

PARAMETER	INNER	OUTER	UNITS
Brushes per sector	7	5	--
Number of sectors	22	38	--
Brush contact area (apparent)	2.18	2.18	cm^2
Brushes per rotor	616	760	--
Maximum current per brush	4.55	3.68	kA
Slip ring diameter	30.48	76.2	cm
Slip ring length	10.16	6.35	cm
Slip ring speed	106	220	m/s
Slip ring area	766.5	1,140	cm^2
Strap thickness	0.236	0.236	cm
Strap width	1.14	1.14	cm
Brush current density	2.09	1.69	kA/cm^2
Strap current density	16.83	13.64	kA/cm^2
Slip ring current density	0.91	0.61	kA/cm^2

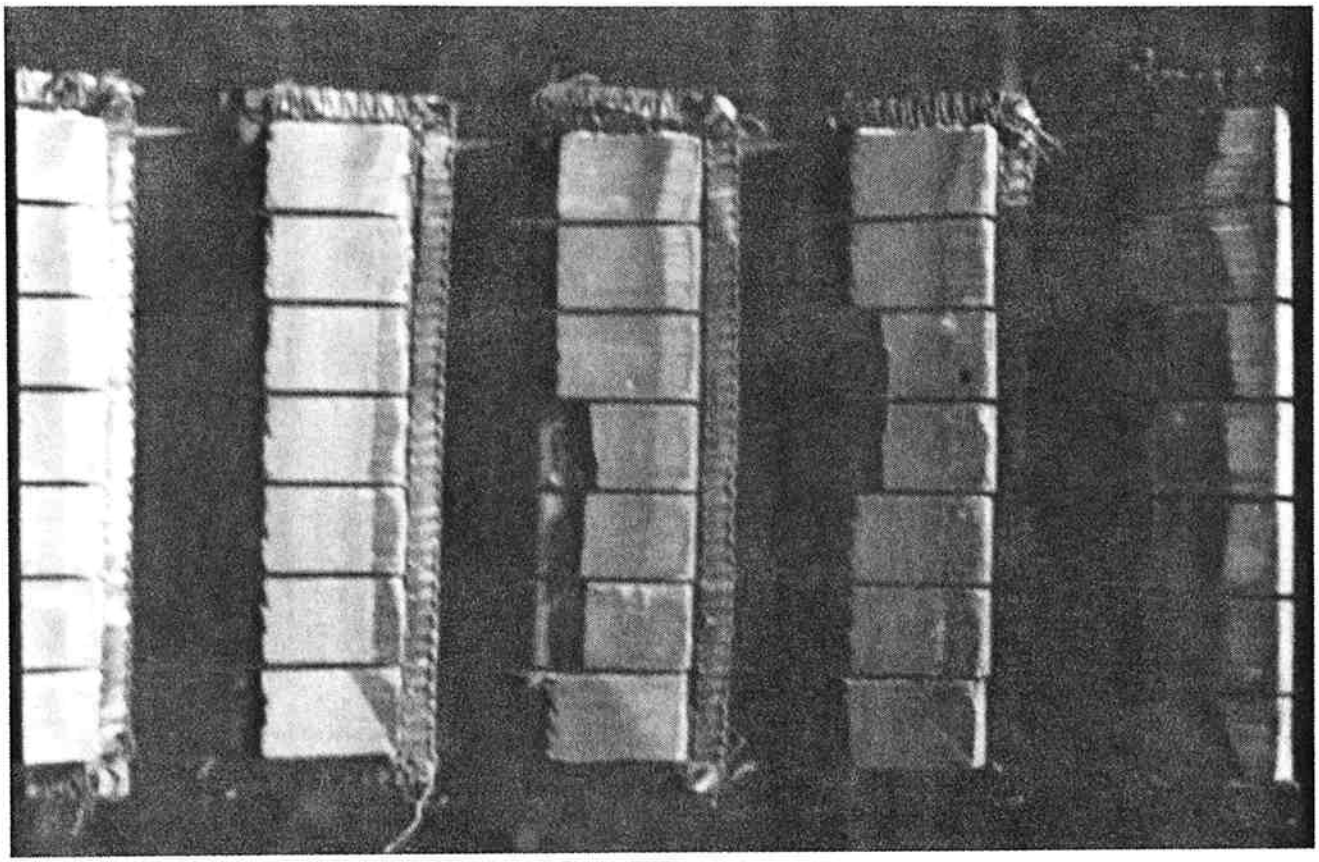

Figure 5. Chattering damage, original inner armature brushes

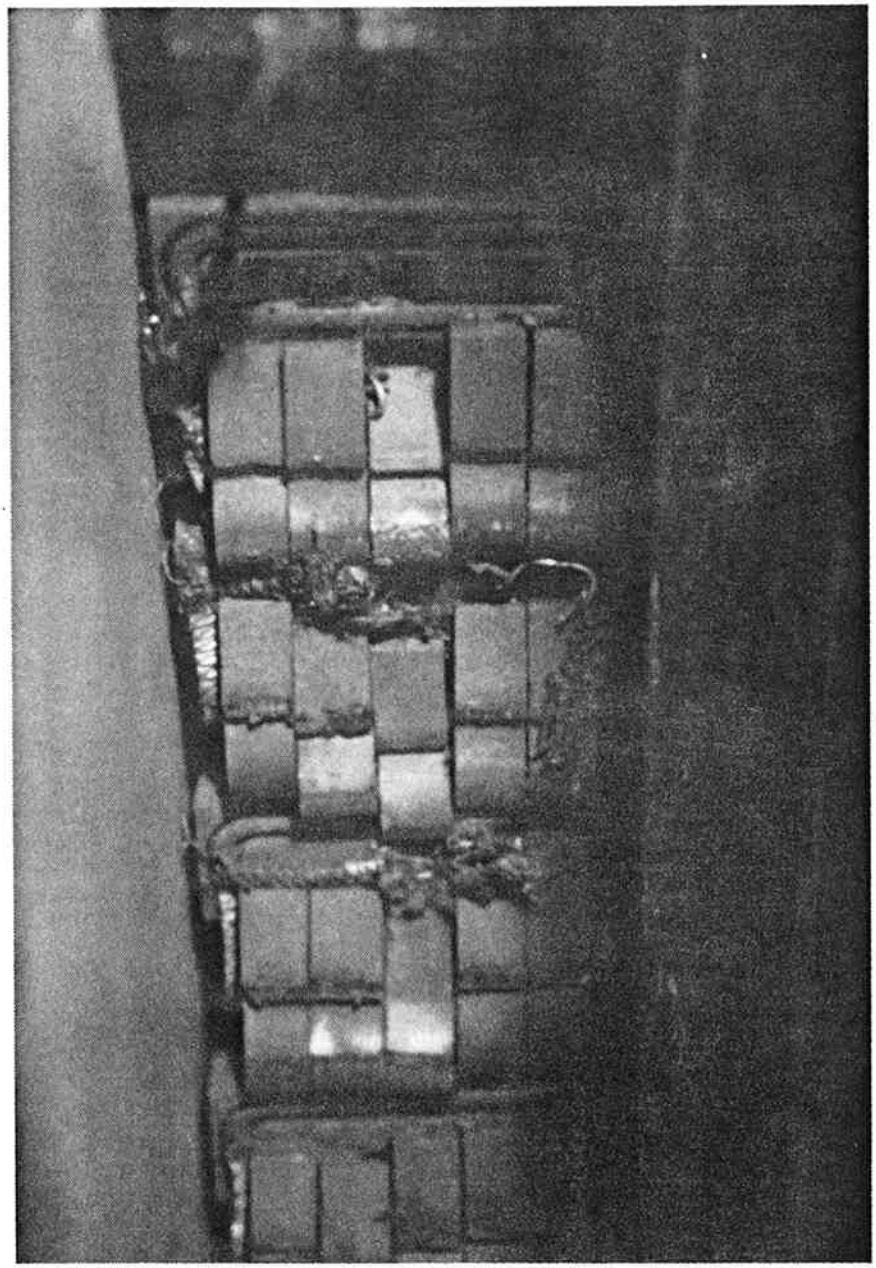

Figure 6. Strap bending damage, original outer armature brushes

For the original inner design, the self-compensation force due to the fixed geometry compensating turn was calculated from empirical handbook data[2] using the relation

$$F = 5.4\ k\ (I^2/d)\ x\ 10^{-7}\ \ lbf/ft,$$

where k is a geometric shape factor found from conductor size and spacing, and d is conductor separation in inches. Solving this relation yeilds a total force

$$F_b = 59.81\ N.$$

Treating the brush strap as a simply supported beam and resolving the normal component of the reaction at the contact yields

$$R_b = 23.25\ N\ (radially\ downward).$$

The Lorentz force on the brush strap due to external field is a body force

$$F_e = \iiint \overline{J} \times \overline{B}\ dv.$$

For simple, uniform, rigid conductors and uniform, steady state $\overline{B}$, the total instantaneous magnitude of force is

$$F_e = IBl,$$

where l is the length of the conductor in meters. The direction of F_e is found by the right hand rule. Substituting for full current and field conditions at the inner rotor of the generator yields

$$F_e = 663.8\ N.$$

Again treating this as a centric load on a simply supported beam, and resolving the normal component of the reaction at the contact, yeilds

$$R_e = 257.9\ N\ (radially\ upward).$$

The actuator force, which is applied directly to the sliding contact, is

$$F_e = 57.8 \text{ N (downward)}.$$

The total reaction at the contact must be positive (downward) for stable current transfer. Expressing this resultant, using the model presented here, as a quadratic equation in I (assuming full excitation) indicates that the resultant reaches zero at a total machine current of approximately 98.3 kA. Current interruption due to inner brush chatter was observed during testing at 80-90 kA at 4 T excitation.

The original outer current collector was uncompensated because normal current direction results in a Lorentz force in the brush strap that aids in downward load at the sliding contact--

$$R_e = 140.8 \text{ N}$$

(at full current and field).

However, the strap cannot withstand the bending stresses associated with this external load. Treating the brush strap as a laminated beam whose yield strength is dominated by the two dispersion strengthened members, finding the distributed load that yields the maximally stressed fiber of this assembly, and solving for the current (at full field) that would create this load, indicates that a total machine current of as little as 100 kA could cause yielding in bending in some straps. This was the method used to infer the magnitude of the fault current that resulted in the observed strap bending damage.

New Design Constraints

Any new current collection system for the HVHPG would require significant and costly modifications to the stator subassembly unless the following constraints are applied:

1. the existing molded, elastomeric, bellows type actuators must be used as the brushgear actuators,
2. these actuators must reside at their original radial and azimuthal locations within the stator cavities so that the existing high pressure gas feed ports can be used, and
3. no machining of the stator or its components should be involved, so as to preserve the integrity of the insulation.

In addition, because brush packing factor cannot be reduced significantly if the machine is to keep its 700 kA current rating, the approximate number, size, and shape of the sliding contacts are essentially frozen. Finally, to enable the HVHPG to power underdamped inductive loads, a redesigned current collection system should be able to withstand current and direction reversals.

Design Concepts

Numerous concepts for redesigned armature brushgear sets were evaluated. A completely compensated armature from the slip ring to the collecting ring is not possible because an odd number of turns is required to close the circuit. A design in which the brush strap itself was fully compensated (fig. 7) was considered. Such a compensation must be accomplished by an

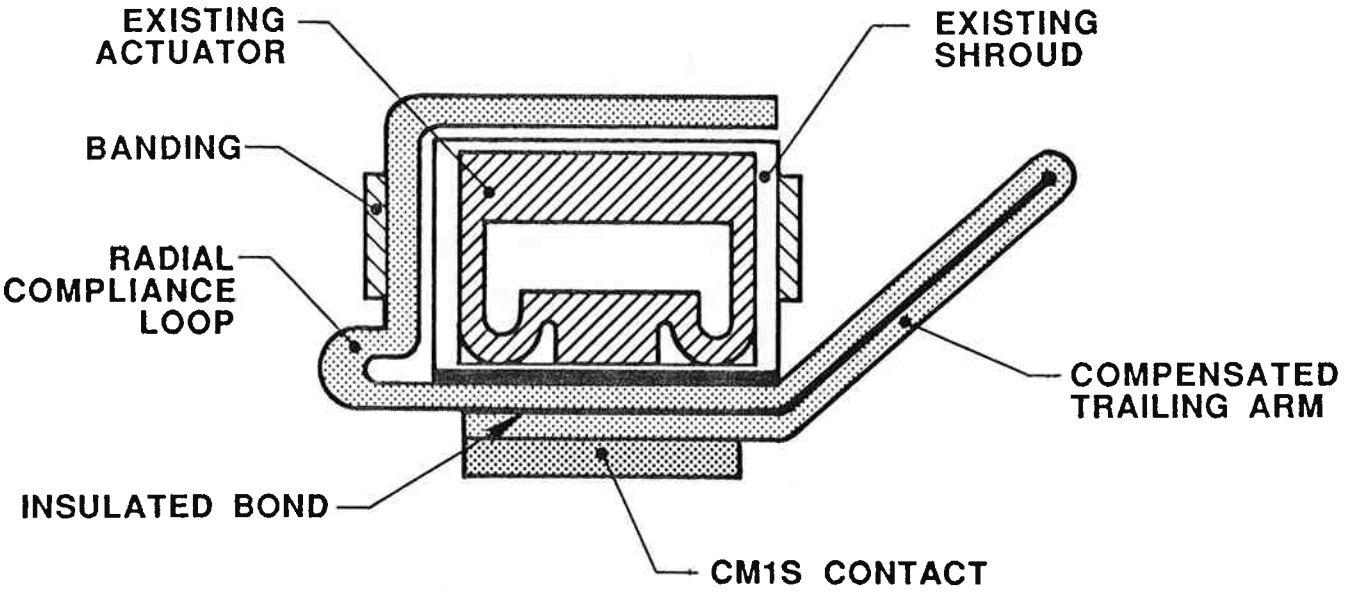

Figure 7. Fully compensated armature brushgear design

insulated bond between the conductors; if not, the separation between the two will allow the external forces to unload the contact, as in the original design. Further-more, any compensating turn must be bonded to itself because the magnetic pressure due to external 5 Tesla fields is larger by about a factor of eight than that due to brush strap current density at rated current. These factors tend to obviate a conducting trailing arm, which would be difficult to anchor, bond, insulate, and actuate. On the other hand, uncompensated designs, which were also evaluated, are inherently one-directional as far as current flow is concerned, so were not pursued.

Resulting from these studies was a compensated, idle trailing arm (CITA) brushgear design (compensated only in the region of the sliding contact). This design, for both the outer and inner rotor slip rings, is shown in figures 8 and 9 respectively. The trailing arm carries no current, so it is not subject to bending or lifting forces. The brush strap is compensated upon itself in the region of the sliding contact in order to minimize the effects of external forces on contact load.

This effect is imperfect, resulting in reduced current rating in the reversal mode. This is because an external, uncompensated, radial compliance loop is required for contact actuation. Normal current direction loads this loop as a thin walled pressure vessel, resulting in an extra radial load at the contact. Therefore, these designs are biased so that peak reactions to external forces at the contacts, in the full normal current condition, enhance contact loading, thus guarding against any armature instability as encountered before in resistive load testing.

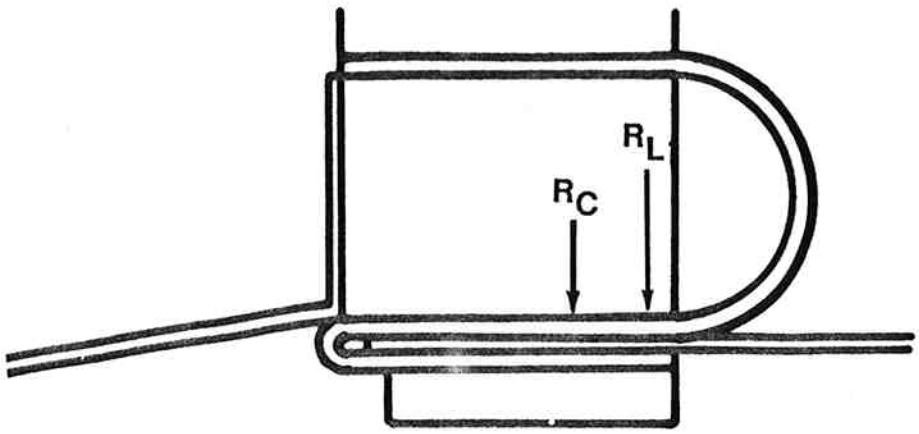

Figure 8. Compensated, idle trailing arm brushgear design (outer)

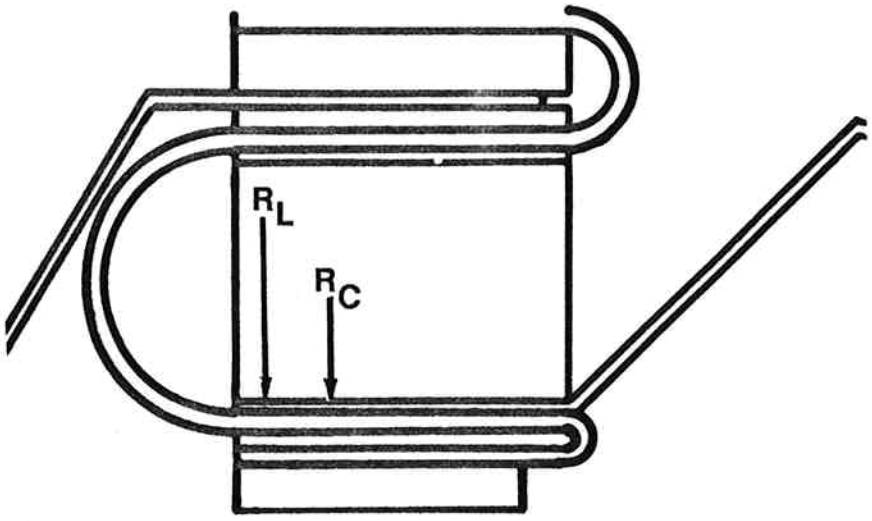

Figure 9. Compensated, idle trailing arm brushgear design (inner)

Analysis of the Compensated, Idle Trailing Arm Design

Thermal and Mechanical. The CITA design was analyzed for various performance criteria. For a single full current discharge into a resistive load, a temperature excursion of 25°C in the radial compliance loop was considered acceptable. Assuming the lamination of the main conductor to be made up of 0.013 cm copper shims, carrying continuous peak current for the entire pulse duration of 40 milliseconds, at constant (room temperature) resistivity, and sharing current equally, a total of nine such shims was determined. Next, the minimum radius of the radial compliance loop, for radial actuation capability, was determined. Assuming an average brush wear and thus allowing for the actuation travel, the lamination was modeled according to Castigliano's theorem for radial spring constant. This analysis determined that an inner shim radius of 0.67 cm would result in an effective spring rate (neglecting transverse shear due to friction) such that the resulting contact load at determined wear will yeild 1.3 grams per ampere of transferred current, an accepted rule of thumb[3]. As an adjustment against the assumption of no transverse shear, this radius was increased to 0.76 cm, to take advantage of the radial height of the actuator shroud. The resulting reactions to all forces at the sliding contact, at full normal direction current, are given in table 3.

Electromagnetic. Force analysis for the CITA current collectors concentrated on two main external forces: the force due to net (uncompensated) $\bar{J}$ in the bonded compensating turn directly above the sliding contact, (R_C) and

Table 3. Summary of Compensated, Idle Trailing Arm (CITA) forces (at full current in normal direction)

FORCE	DESCRIPTION	MAGNITUDE (N)	
		INNER	OUTER
F_a	Applied actuator force	57.8 ↓	57.8 ↓
R_c	Reaction at contact due to incomplete compensation from contact to strap	140.4 ↓	173.2 ↓
R_1	Reaction at contact due to external forces on radial compliance loop	126.3 ↓	155.8 ↓
f	Frictional force on contact (μ = 0.3)	97.4 ←	116.0 ←
F_s	Total force reacted by idle trailing arm	155.2 (tensile)	604.7 (compressive)
R_s	Radial reaction at contact due to F_s	none	427.6 ↑

the reaction at the sliding contact due to external forces on the radial compliance loop (R_1). In both cases, the CITA design is based on using these

Net J in the contact/compensating turn region will be a strong function of the seating point of the contact on the slip ring, and resistive and inductive diffusion of current from the contact to the compensating turn. Assuming that only 50% of the current is compensated upon itself effectively, an estimated R_C, radially downward during normal current flow, was calculated for both

The circuit from brush to compensating turn was modeled to determine if a resistive insert could be used to force better current penetration into the compensating turn (figure 10). An input current waveform was modeled to simulate a full current pulse. This linear, lumped parameter circuit was solved by code.[4] Stainless steel was used as the resistive insert. Figure 11 shows the insensitivity of current division between paths A and B as a function of the thickness of the resistive insert. This result is due to the fact that the copper graphite composite material (Morganite CM1S™) itself is relatively resistive (ρ = 38.1 $\mu\Omega$-cm), making simple resistive current division ineffective. An insulating insert could be used to force the issue, but would

The reaction to radial compliance loop force was found by treating the laminated loop as a thin walled pressure vessel and calculating the radial load reacted at the contact. Again, this force assists contact load in normal operation. These forces are presented in table 3.

Other Force Considerations. Summing the radial loads at the contact, and assuming a coefficient of friction between the copper-graphite contact and the plasma sprayed copper slip ring of 0.3, yields predicted frictional forces.

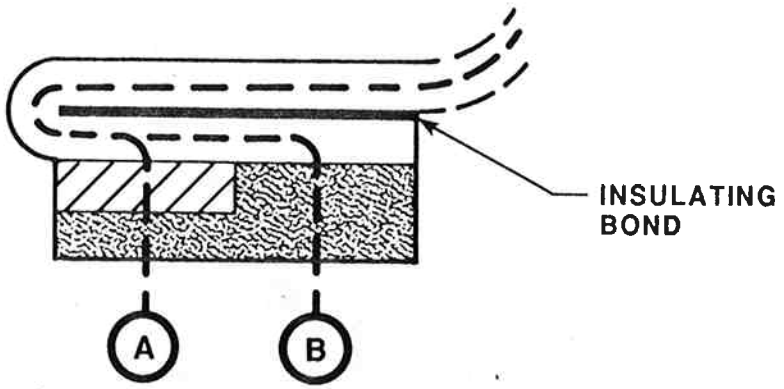

Figure 10. Sliding contact resistive insert concept

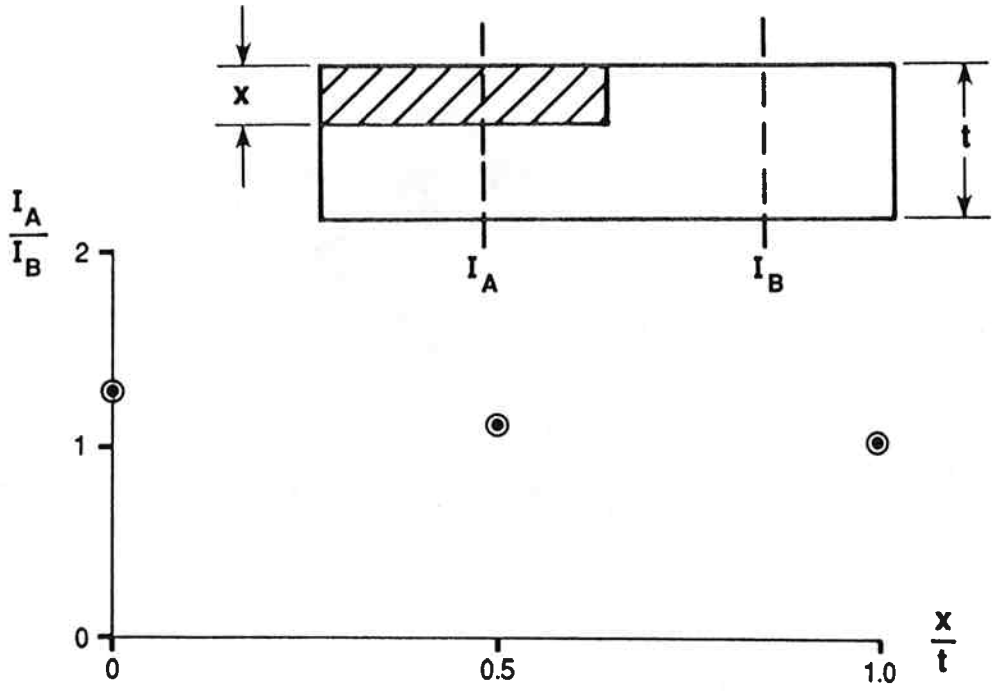

Figure 11. Current diffusion from contact to strap as a function of insert height

Considering these forces along with the azimuthal component of the radial compliance loop external force, the total strap reactions are estimated; these forces are also shown in table 3. In the outer design, the idle arm is actually loaded in compression for a period of time around peak current. However, the arm as a whole behaves as a compression member rather than a slender column, so buckling will not occur. Also, the magnitude of the resulting compressive stress is small compared to yield stress in the arm material (316 stainless steel). However, the dynamic stability of a "leading" arm brush has not been studied in depth. Finally, the friction force and the arm reaction act to create a couple on the contact. This couple is proportional to brush thickness, indicating that a tradeoff between brush life and mechanical performance may be required.

At the inner radius, another, potentially more serious, feature exists. The topology and geometry of the HVHPG make this pole of current collection less convenient than that at the outer diameter. The steep angle contained between the arm and the azimuth results in a radially upward reaction at the contact due to arm tension. If this force is sufficient to raise the heel of the contact, the toe will be loaded with a correspondingly higher load. Toe contact with the slip ring enhances current compensation, reducing overall force, but asymmetrical wear might result, limiting brush life. Numerous design modifications are being evaluated to correct this feature.

The degree to which this current collection system can operate with reversal current is strongly dependent on the amount of compensation achieved in the turn at the sliding contact. Using the same current

penetration model that was used to estimate the R_C forces, it is estimated that a peak reversal current of 50 to 100 kA might be conducted without contact instability.

Prototype Fabrication

A full scale prototype of the outer CITA brushgear design has been fabricated and assembled into an HVHPG current collector ring (fig. 12). This laminated copper shim bundle was formed by hand: a tool and die set has been designed for mass production. The compensating turn joint was formed by propane-acetylene torch brazing with a nickle based metallic glass paste-form brazing alloy (Metglas 2005™). Migration of this brazement filler into the radial compliance region of the lamination was blocked by an anti-wicking compound. The copper graphite composite contact pads (Morganite CM1S™) were joined to the copper lamination, by the same brazement filler, in the same setup.

Although prototype laminated shunts for the inner CITA brushgear design have been formed and assembled, this design is subject to further review because of the steep angle of the idle trailing arm, as discussed earlier.

Motoring Current Collection System

Original Design

As mentioned above, a cantilever, spring-actuated motoring brush failed in previous testing of the machine. This brush is illustrated in figure 13. Two reasons for the failure have already been put forward: (1) the brushes

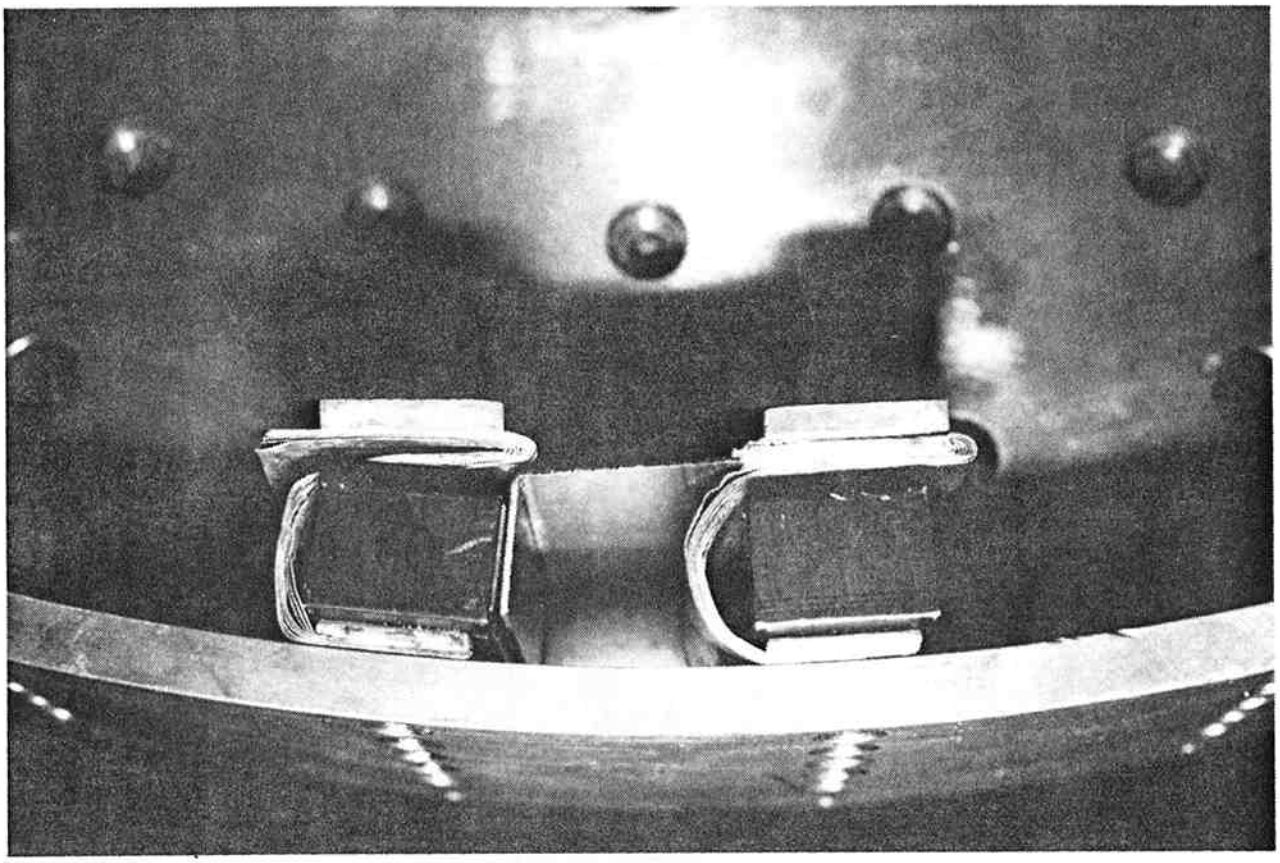

Figure 12. Prototype outer compensated, idle trailing arm collector

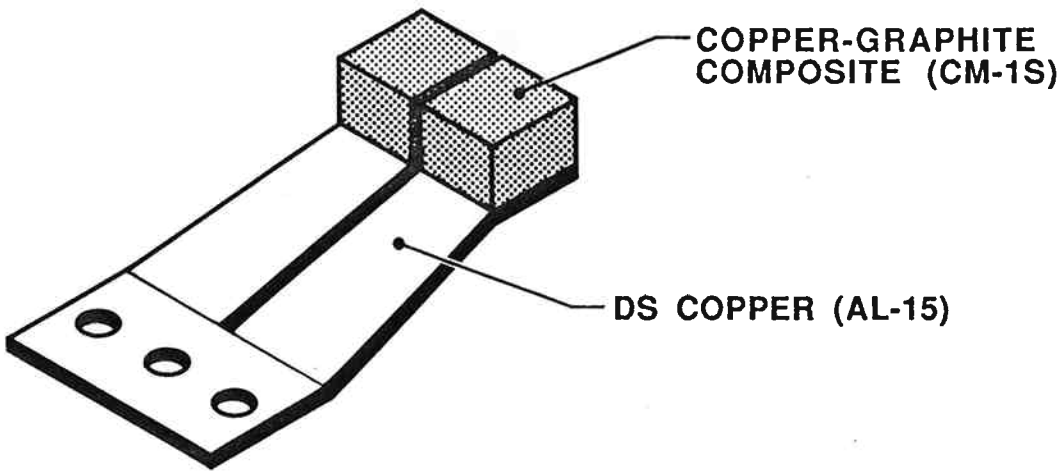

Figure 13. Cantilever brushstrap showing field, current, and force directions

were unable to withstand the azimuthal Lorentz force generated during normal or fault current operations, and (2) wear of the brush contributed to low contact force, high contact temperature, and eventual failure.

The first failure mechanism is demonstrated in figure 14, which shows the discharge path in cross-section. Analysis indicates that the motoring brush design was adequate to withstand normal external forces, but fault currents were of concern. Apparently the air gap insulation between the motoring brush mounting plate and the bearing housing was compromised by a buildup of brush debris. This contact created a fault path which was closed by actuating the number 1 outer brush set during the final emergency shutdown of the machine. This fault path was confirmed by observing arc damage to both the bearing housing and mounting plate, and the current was sufficient to destroy the motoring brushes, thus preventing a measurement of pre-failure wear.

The contribution of brush wear to brush failure became a matter of concern because of the duty cycle for the copper graphite composite motoring brushes. The current density and slip speed of the brush material far exceeded the manufacturer's specification for continuous duty, as well as previous experience with this material at CEM-UT. Table 4 summarizes these paramters and points out the intermittent nature of the present application.

The brush wear related failure mechanism is supported by figure 15, which shows the relationship between contact force and brush wear. If a brush wore more than about 0.63 mm (0.025 in.) the coil spring would actually have been working against the brushstrap to establish contact. This is obviously an undesirable situation, especially since the spring rate of the cantilever

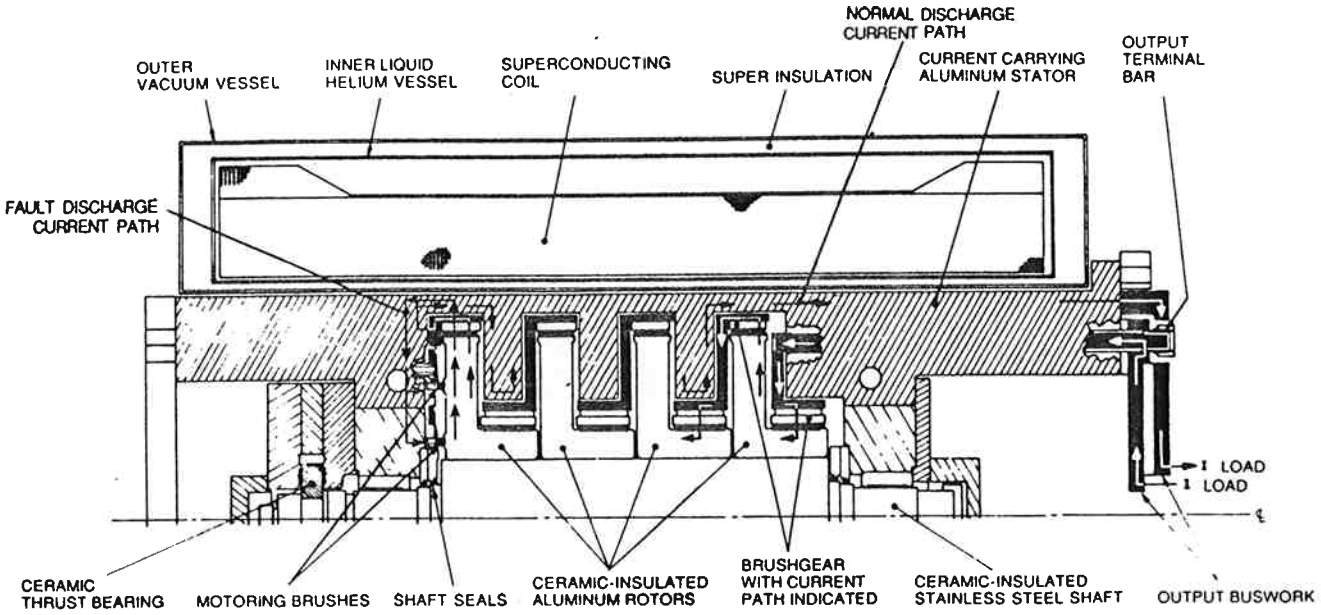

Figure 14. Fault current path

Table 4. Copper graphite motoring contact characteristics

	SLIP SPEED (m/s)	CURRENT DENSITY (kA/m^2)	MOTORING TIME (s)
MANUFACTURER'S CONTINUOUS DUTY RATING	25	194	Continuous Duty
DUTY ENCOUNTERED IN SELF-MOTORING IRON CORE HPG'S	150	372	≈250
DUTY REQUIRED IN MOTORING THE HVHPG	162	1,160	≈30

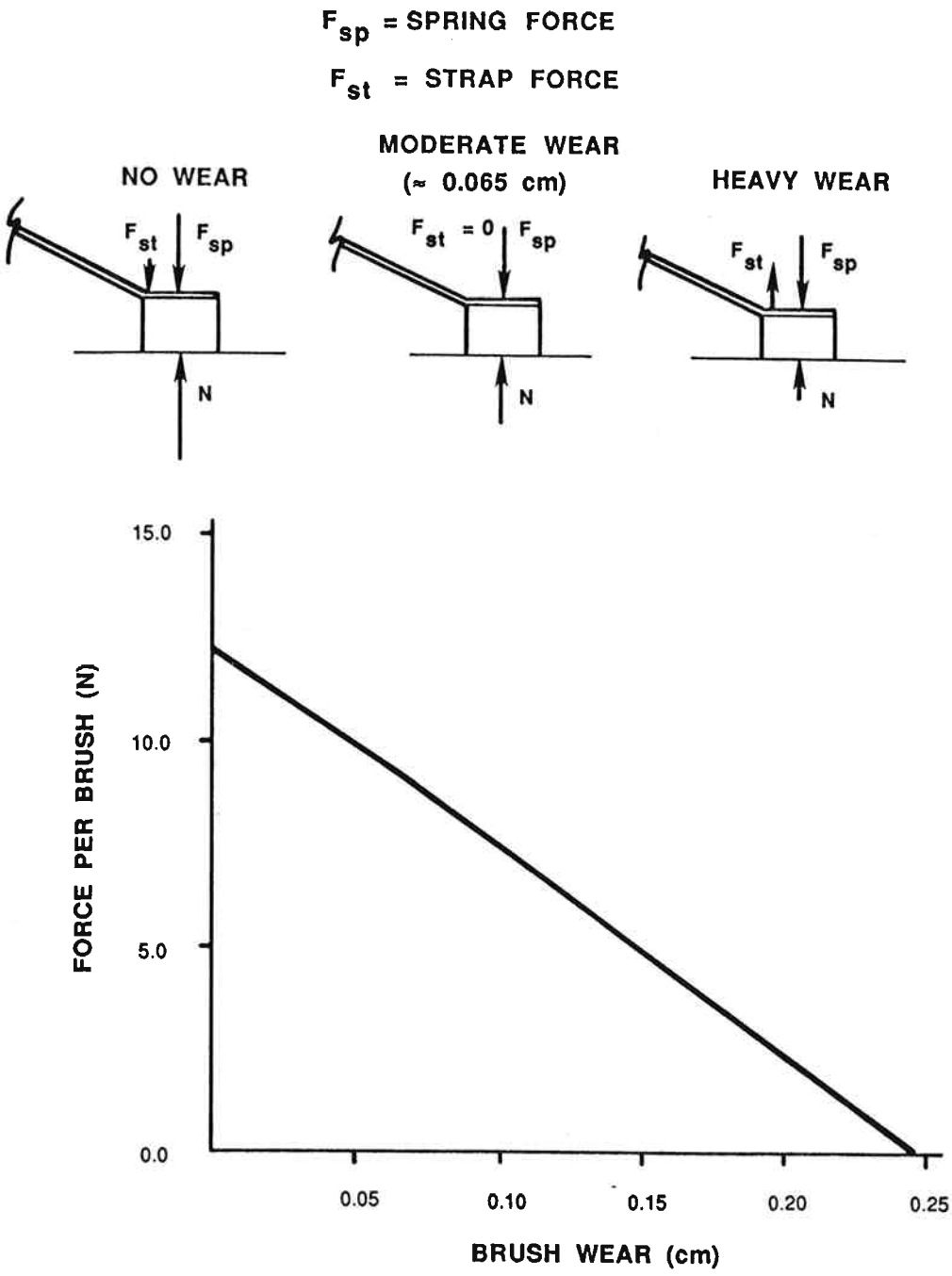

Figure 15. Brush wear produces low contact forces

brushstrap was about 8 times that of the coil spring. In fact, with wear of about 2.5 mm (0.1 in.) the contact force would drop to zero. A lower contact force in turn produces a higher voltage drop and higher temperature at the brush/rotor interface.

Figure 16 shows the results of static thermal tests performed on the cantilever brushgear. In this test, 200 A passed for 60 s through each brush to a stationary steel block while the temperature profile was recorded by an infrared camera. The peak temperature after 60 s, which always occurred at the brush/block interface, was recorded and appears in figure 16. Even though 60 s is about twice as long as the typical motoring time of the HVHPG, it is possible that motoring brush temperatures reached the values shown here since the static test neglects the frictional component of heating. The test demonstrates the nearly exponential rise in temperature which occurs at low contact forces. At a very low force (1.1 N) arcing was in fact observed at the interface.

As a result of all these factors, it is reasonable to assume that, while motoring to 4,000 rpm in the final test of the HVHPG, one or more motoring contacts failed due to excessive wear. The resulting overheating caused mechanical failure that was audible to the field operator, who radioed instructions for an emergency shutdown. This action closed the observed fault current path, which completed the damage to the motoring brushgear.

Design Constraints

It would be relatively simple to design a brush to overcome the problems of Lorentz force loading and brush wear were it not for the

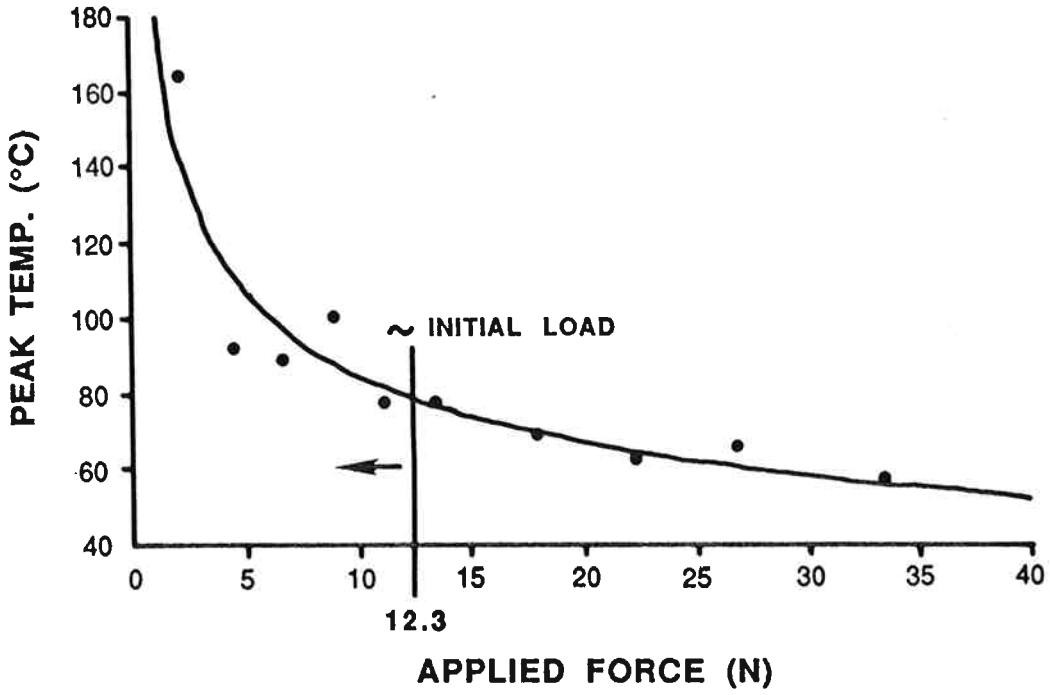

Figure 16. Low contact forces contribute to high brush temperatures

constraints imposed by the machine geometry. Ideally the current should be collected axially--that is, parallel to the magnetic field vector--to minimize J x B loads. Also, the brush should provide relatively constant actuation force (zero spring rate) in spite of brush wear. A brush block with a constant force actuating spring would be ideally suited for such an application (fig. 17). This brush arrangement is often used for continuous duty applications in electric motors. In the HVHPG, however, the total axial distance from rotor face to stator is only 3.8 cm. Since brush blocks are considerably larger than this (the spring alone would need to be about 2 to 3 cm in diameter and has to unravel an additional diameter before exhibiting constant force characteristics), this alternative could not be used for a new motoring brush.

Hinged Brushstrap

The final design of the motoring brushes calls for a hinged, laminated strap as shown in figure 18. This design separates the current collection and load-carrying functions of the brush assembly. It is still susceptible to Lorentz force sideloading, but since the reacting members (the hinge, pivot arm, and mounting plate) no longer need to be flexible, they can be enlarged for strength. Flexibility and current collection are obtained through the ten laminations of 0.13 mm (0.005 in.) copper shim stock. A spring rate for the newly designed strap was calculated to be about 0.38 N/mm (2.18 lb/in.), as opposed to around 8.76 N/mm for the old brushstrap. These rates are compared in figure 19, which shows that even if the brush wears considerably it should still have an adequate actuating force.

Figure 17. Brush block with constant force actuating spring

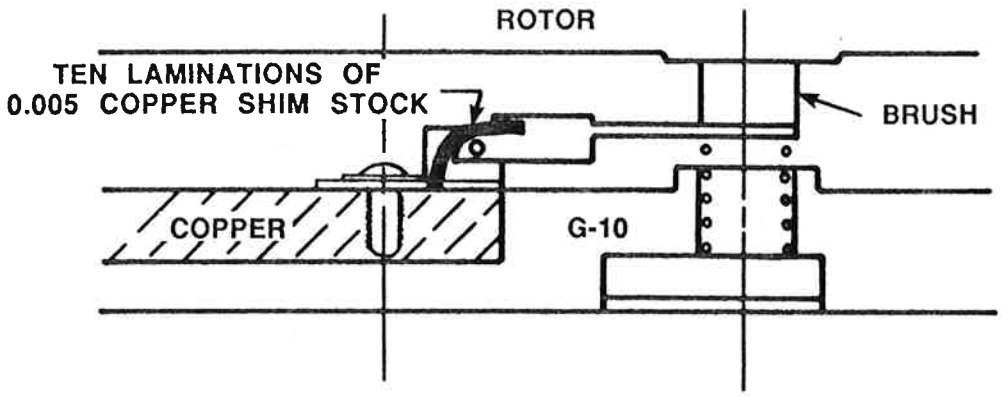

Figure 18. Hinged, laminated brush assembly

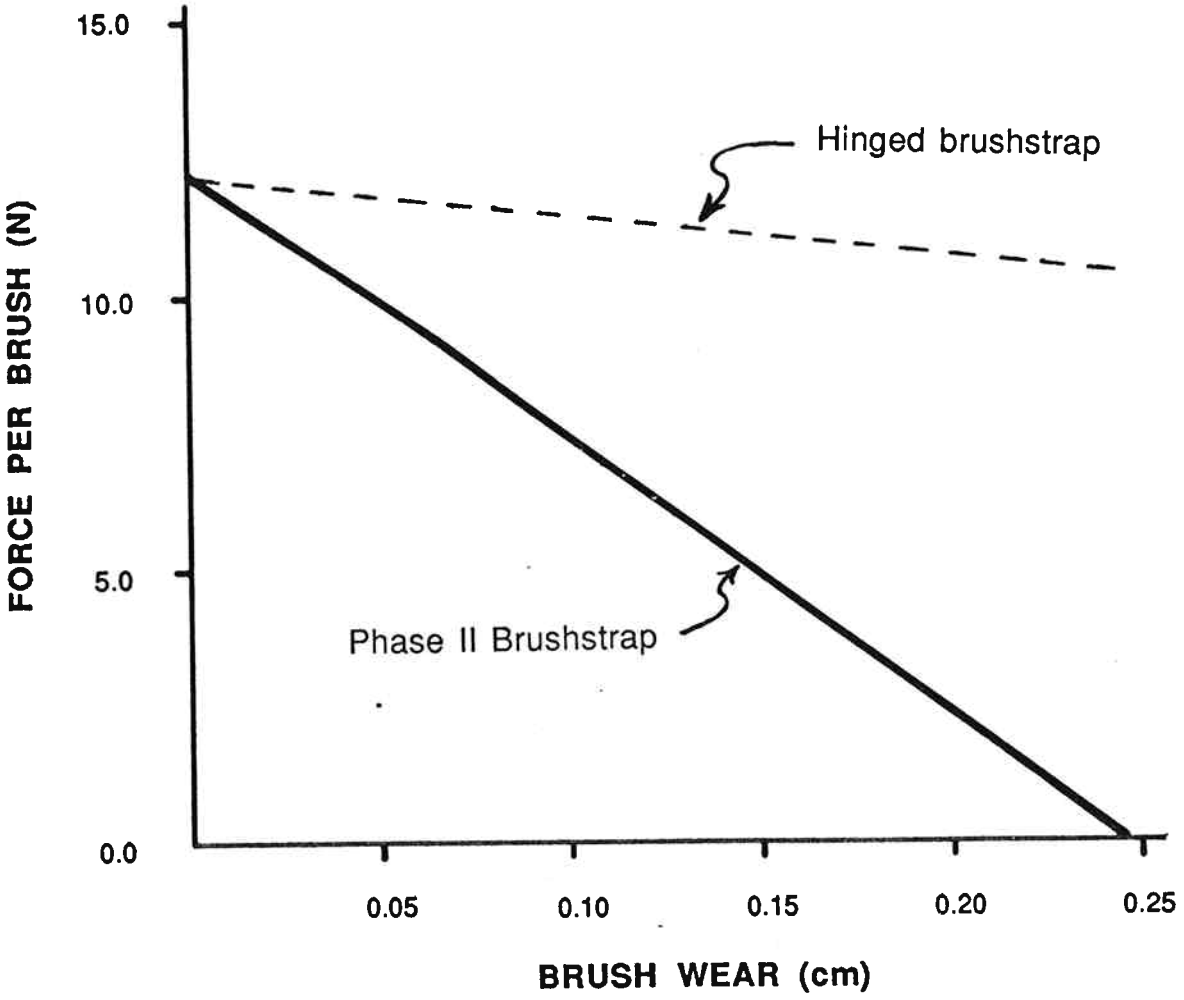

Figure 19. Comparison of effect of brush wear on contact force for old and new designs

Prototype Testing

In order to evaluate the performance of the hinged motoring brush, several prototypes have been built and will be tested on a Sliding Electrical Contact Tester (SECT). This device is discussed in a companion paper[5]. The SECT is capable of reproducing the rotational and electrical aspects of the actual HVHPG, but not the magnetic field. It consists of a steel rotor with a face-mounted aluminum insert against which the prototype brushes will ride. The insert, with its plasma-sprayed copper slip rings, is shown in figure 20. It and the stator of the SECT simulate the rotor and mounting plate of the HVHPG during motoring to 6,000 rpm (165 m/s). Like the static test described earlier, temperature profiles will be recorded with an infrared imager and actuating force will be varied. Also, brush-rotor voltage drop will be measured.

Conclusions

A high voltage, air core, high external field homopolar generator has been built and tested at the Center for Electromechanics, The University of Texas at Austin. Such machines are important for enhanced energy storage density applications, or where powering electromanetic launchers without intermediate energy storage and conditioning is required. Valuable data in current collection in high external fields was gathered during these tests. Based on this experience, new designs for motoring and armature current collection systems have evolved. Prototypes of these sytems have been built, and some are scheduled for testing in real conditions except for high external field.

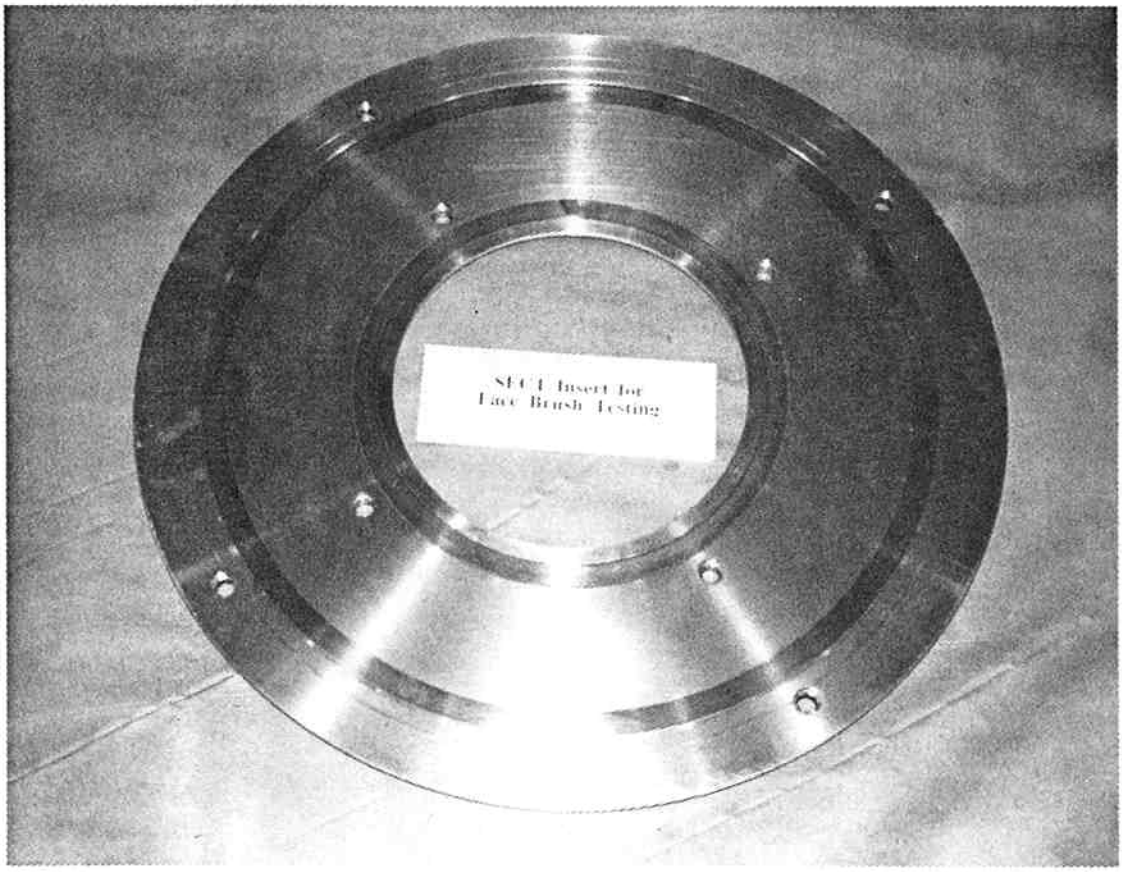

Figure 20. Face-mounted insert for the SECT showing copper slip rings

The high voltage homopolar generator is being maintained in a disassembled state for future testing of these improved designs.

Acknowledgments

The work reported herein was conducted under U. S. Army Armament Research, Development, and Engineering Center and Defense Advanced Research Projects Agnecy Contract Number DAAA21-85-C-0210. The high voltage homopolar generator was designed and constructed by the Center for Electromechanics, The University of Texas at Austin, under GA Technologies, Inc., Contract Number SC006678. The superconducting field coil for the high voltage homopolar generator was designed and constructed by GA Technologies, Inc. CM1S is a trademark of Morganite, Incorporated. Metglas is a trademark of the Allied corporation.

References

1. J. H. Price and J. H. Gully, "The High Voltage Homopolar Generator," presented at the 3rd Symposium on Electromagnetic Launch Technology, Austin, Texas, April 20-24, 1986.

2. ALCOA Aluminum Bus Conductor Handbook, Aluminum Company of America, Pittsburgh, Pennsylvania, 1957.

3. R. A. Marshall, "High Current and High Current Density Pulse Tests of Brushes and Collectors for Homopolar Energy Stores," presented at the 26th Annual Meeting of the Holm Conference on Electrical Contact, September 29-October 1, 1980.

4. SPICE, version 2c.1, University of California at Berkeley, E. Cohen and D. O. Pederson, March 31, 1976.

5. R. L. Laughlin, J. H. Gully, and M. L. Spann, "Design and Testing of a Continuous Duty Current Collectors", presented at the 1987 International Current Collector Conference, Austin, Texas November 16-17, 1987